

Tunable photon heat amplification in two-dimensional materials

Hamidreza Simchi*

Department of Physics, Iran University of Science and Technology, Narmak, Tehran 16844, Iran and Semiconductor Technology Center, P.O.Box 19575-199, Tehran, Iran

(Dated: December 3, 2024)

We study the photon heat tunneling across a stratified media made by graphene (G) and/or molybdenum disulfide (MoS_2). The free energy of fluctuating modes depends not only on the number of G/MoS_2 layers but also on the priority of graphene layer respect to MoS_2 layer in the media. The rule is; the thinner layer should be the nearest neighborhood of leftmost and rightmost sides of the media for getting the highest interaction free energy. The free energy can be tuned by applying an external gate voltage to MoS_2 layers due to the tunable property of the dielectric constant of MoS_2 by gate voltage. In the *silicon/MoS₂/silicon* three-body configuration, the photon heat tunneling is amplified significantly due to the increasing the number of the coupled modes. Due to the amplifying effect, this mechanism could be exploited to improving detection ability in the near infrared detection systems.

I. INTRODUCTION

A semiconductor photovoltaic (PV) cell absorbs photons and generates hole-electron pairs. All photons, with energy less than the energy gap (E_g) of semiconductor, are only dissipated into heat within the atomic lattice and do not contribute in the pair generation. Some parts of photons with energy larger than E_g are converted to electron-hole pairs but some parts of their energy is dissipated via phonon excitation. A body at temperature T radiates electromagnetic waves due to the thermal and quantum fluctuations[1–4]. By defining the thermal wavelength as $\lambda_{th} = \hbar c / (k_B T)$, we can consider two different regimes for heat flow. At distances smaller than λ_{th} the evanescent term of heat flow dominates (near-field) and for distances larger than λ_{th} , the propagating radiation term dominates (far-field) [1–6]. Hence, the near-field thermal radiation confined on the surface is potentially important source of energy. Now if we consider a PV cell in proximity of a thermal emitter, the energy can be extracted when the evanescent photons tunnel toward the cell. Such device has been proposed less than twenty years ago and is called near-field thermophotovoltaic (NTPV) system [7].

It has been shown that, the near-field heat transfer between two plates varies as d^{-2} where d is vacuum gap between the plates [2, 8–10]. It should be noted that the d^{-2} dependence is for contribution from p-polarized electromagnetic waves only since the contribution from s-polarized waves will asymptotically reach a constant as $d \rightarrow 0$ [11, 12]. For heavily doped semiconductors, the contribution of p-polarized waves dominates over that of s-polarized waves when $d < 10$ nano-meter (nm)[13] but for metals the crossover can take place at much shorter distances [14, 15]. It has been shown that, there are optimal values of real and imaginary parts of the dielectric constants of plates, which for them, the near-field heat transfer is maximized[16]. Messina et al., have

introduced the concept of three-body amplification of heat exchanged at nanoscale between two media[17]. We have shown that, how one can overcome the limitations of Messina’s model[17] by using graphene as intermediate layer[18].Of course, the theory of van der Waals forces can be generalized to different multilayer geometries and a closed form solution that explicitly depend on the number of layers in the multilayer system can be derived[19, 20].

In this paper, we consider a multilayer structure of graphene and/or MoS_2 and study the evanescent photon heat tunneling across the multilayer. We show how the free energy flux depends not only on the number of layers but also on the priority of graphene layer respect to MoS_2 layer in the stratified media. There is a rule. The thinner layer should be the nearest neighborhood of leftmost and rightmost sides of stratified media for getting the highest interaction energy. Since the dielectric constant of MoS_2 can be tuned by applying an external gate voltage (V_g), we show how one can tune the photon heat tunneling across the multilayer structure by applying (V_g). For showing the probable application of heat flow, we consider a three-body configuration as *silicon/MoS₂/silicon*, and show how the detection ability in near infrared region increases when we add the intermediate MoS_2 layer. The structure of article is as follows: In section II, the calculation model is explained. In section III, the numerical calculation, results and discussion are provided. The summary is presented in section IV.

II. CALCULATION METHOD

In this section, we discuss about dielectric constant of MoS_2 , and graphene, firstly. Then, we study the photon heat tunneling in multilayer structures and derive the closed form of free energy density in terms of the number of layers. Finally, we review the heat flow amplification in three-body configuration shortly, based on our previous work [18].

* simchi@alumni.iust.ac.ir

A. Dielectric constant of MoS_2

A large range of value for dielectric constant (ϵ) of MoS_2 has been found in experiments [21–25]. It has been shown that ϵ can be manipulated by an external electric field[26]. Mukherjee et al., have studied the complex electrical permittivity of monolayer MoS_2 in near and visible range[27]. They have shown that the real and imaginary part of ϵ can be written as[27]:

$$\epsilon_R = \epsilon_\infty + \frac{137}{\pi} \sum_{j=0}^5 \frac{a_j \omega_P^2}{(\omega_j^2 - \omega^2)^2 + \omega^2 b_j^2} (\omega_j^2 - \omega^2) \quad (1)$$

$$\epsilon_I = \frac{137}{\pi} \sum_{j=0}^5 \frac{a_j \omega_P^2}{(\omega_j^2 - \omega^2)^2 + \omega^2 b_j^2} (\omega^2 b_j) + \alpha \exp\left(-\frac{\omega - \mu}{2\sigma^2}\right) \quad (2)$$

where, $\omega_P = 28.3 \times 10^{-3}$ electron volt (eV), $\epsilon_\infty = 4.44$, $\alpha = 23.224$, $\mu = 2.7723$ (eV), $\sigma = 0.3089$ (eV)[27]. If $a = a_j/\hbar$ (eV), $b = b_j/\hbar$ (eV) and $c = \omega_j/\hbar$ (eV), then the other constants of above equations are given in table I[27]: However, by applying a gate voltage V_g , the Fermi energy E_F changes as[27]

$$E_F = \hbar^2 \pi C V_g / 0.7 m_e e^3 \quad (3)$$

where, $C = 1.2 \times 10^{-8}$ (Fcm^{-2}), m_e and e are mass and charge of electron, respectively. Since, the dependency of constants a_j and b_j to E_F is as follows[27]:

$$a'_j = a_j \exp(-12\pi(E_F - k_B T)^2) \quad (4)$$

$$b'_j = b_j \exp(-12\pi(E_F - k_B T)^2) \quad (5)$$

One can tune the dielectric constant of MoS_2 by applying a gate voltage.

B. Dielectric constant of graphene

It has been shown that, for $q/k_F > \omega/E_F$, the dielectric constant of graphene can be written as[18, 28]:

$$\epsilon(q, i\omega) = 1 + \frac{\pi g c q}{1096 \epsilon_m v \sqrt{q^2 - (i\omega/v)^2}} \quad (6)$$

where, ϵ_m is the average of dielectric constant for the surrounding media, $g = 4$, $c = 3 \times 10^8$ m/s, $v \approx 10^6$ m/s, $k_F = \sqrt{4\pi i \rho/g}$ and ρ is the average electron density [18, 28].

TABLE I: The values of constants of Eqs. 1 and 2.

j	a	b	c
0	2.0089E5	1.0853E - 2	0
1	5.7534E4	5.9099E - 2	1.88
2	8.1496E4	1.1302E - 1	2.03
3	8.2293E4	1.1957E - 1	2.78
4	3.3130E5	2.8322E - 1	2.91
5	4.3906E6	7.8515E - 1	4.31

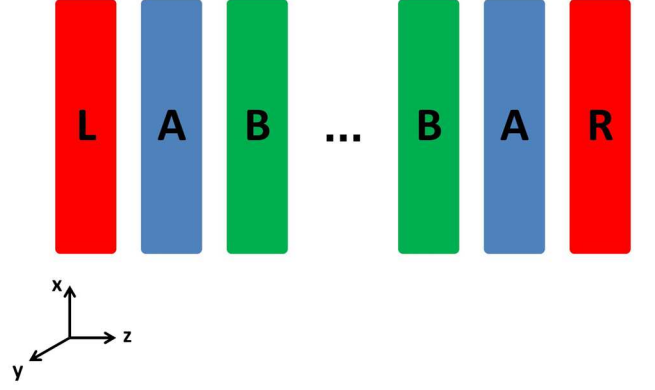


FIG. 1: (Color online) A multilayer slab composed of $N + 1$ layers A and N layers of B .

C. Evanescent photon heat tunneling

Fig.1 shows a multilayer slab composed of $N + 1$ layers A and N layers of B between the semi-infinite region (L) on the left hand side and the semi-infinite region (R) on the right hand side.

We assume the system is homogeneous in (x, y) plane and the electric and magnetic fields have the below form:

$$\vec{E} = \vec{e}(z) e^{i\vec{q} \cdot \vec{\rho}} \quad (7)$$

$$\vec{H} = \vec{h}(z) e^{i\vec{q} \cdot \vec{\rho}} \quad (8)$$

where, $\vec{\rho} = (x, y)$ and $\vec{q} = (q_x, q_y)$. In each dielectric medium i , the function $\vec{e}_i(z)$ must satisfy the Helmholtz equation

$$\frac{d^2 \vec{e}_i}{dz^2} + (\omega^2 \epsilon_i \mu_i / c^2 - q^2) \vec{e}_i = 0 \quad (9)$$

whose solution has the form

$$\vec{e}_i = \vec{A}_i e^{\rho_i z} + \vec{B}_i e^{-\rho_i z} \quad (10)$$

with

$$\rho_i^2 = q^2 - \frac{\epsilon_i \mu_i \omega^2}{c^2} \quad (11)$$

At interface between two neighborhood layers ($i - 1$) and (i), the transverse components of \vec{E} i.e., E_x and E_y , are continuous, while in the longitudinal direction it is the displacement \vec{D} that is continuous i.e.,

$$E_{i-1,x} = E_{i,x}, E_{i-1,y} = E_{i,y} \quad (12)$$

$$D_{i-1,z} = D_{i,z} \quad (13)$$

The same holds also for \vec{B} and \vec{H} . It should be noted that, since both fields are divergence free, the spatial components of \vec{A}_i and \vec{B}_i satisfy the below equations:

$$A_{i,z} = -\frac{i}{\rho_i} (q_x A_{i,x} + q_y A_{i,y}) \quad (14)$$

$$B_{i,z} = \frac{i}{\rho_i} (q_x B_{i,x} + q_y B_{i,y}) \quad (15)$$

which, we use the below identity

$$\nabla \cdot (\psi \vec{a}) = \vec{a} \cdot \nabla \psi + \psi \nabla \cdot \vec{a} \quad (16)$$

By using Eqs. 12, and 13 and also Eqs. 14, and 15, it can be shown that:

$$A_{i,z} e^{\rho_i z} + B_{i,z} e^{-\rho_i z} = \frac{\varepsilon_{i-1}}{\varepsilon_i} \left(\frac{-i}{\rho_{i-1}} \right) (q_x A_{i-1,x} + q_y A_{i-1,y}) e^{\rho_{i-1} z} + \frac{\varepsilon_{i-1}}{\varepsilon_i} \left(\frac{i}{\rho_{i-1}} \right) (q_x B_{i-1,x} + q_y B_{i-1,y}) e^{-\rho_{i-1} z} \quad (17)$$

Also, by using Eq. 12, it can be shown that:

$$-\frac{\rho_i}{i} A_{i,z} e^{\rho_i z} + \frac{\rho_i}{i} B_{i,z} e^{\rho_i z} = (q_x A_{i-1,x} + q_y A_{i-1,y}) e^{\rho_{i-1} z} + (q_x B_{i-1,x} + q_y B_{i-1,y}) e^{-\rho_{i-1} z} \quad (18)$$

Therefore,

$$B_{i,z} = \frac{\varepsilon_i \rho_{i-1} + \varepsilon_{i-1} \rho_i}{2 \rho_i \varepsilon_i} \left[\left(\frac{\rho_i \varepsilon_{i-1} - \varepsilon_i \rho_{i-1}}{\varepsilon_i \rho_{i-1} + \rho_i \varepsilon_{i-1}} \right) A_{i-1,z} e^{\rho_{i-1} z_{i-1} + \rho_i z_i} + B_{i-1,z} e^{\rho_i z_i - \rho_{i-1} z_{i-1}} \right] \quad (19)$$

and

$$A_{i,z} = \frac{\varepsilon_i \rho_{i-1} + \varepsilon_{i-1} \rho_i}{2 \rho_i \varepsilon_i} \left[\left(\frac{\rho_i \varepsilon_{i-1} - \varepsilon_i \rho_{i-1}}{\varepsilon_i \rho_{i-1} - \rho_i \varepsilon_{i-1}} \right) B_{i-1,z} e^{\rho_{i-1} z_{i-1} - \rho_i z_i} + A_{i-1,z} e^{-\rho_i z_i - \rho_{i-1} z_{i-1}} \right] \quad (20)$$

By using Eqs. 19 and 20 it can be shown that[19]

$$\begin{pmatrix} A_{i,z} \\ B_{i,z} \end{pmatrix} = \begin{pmatrix} 1 & -\Delta_{i-1,i} e^{-2\rho_{i-1} d_{i-1}} \\ -\Delta_{i-1,i} & e^{-2\rho_{i-1} d_{i-1}} \end{pmatrix} \begin{pmatrix} A_{i-1,z} \\ B_{i-1,z} \end{pmatrix} \quad (21)$$

where, $d_{i-1} = l_{i-1,i} - l_{i-2,i-1}$ and l_i is the position of the discontinuity the i th and the $i-1$ st layers. Also,

$$\Delta_{i-1,i} = \frac{\varepsilon_{i-1} \rho_i - \varepsilon_i \rho_{i-1}}{\varepsilon_{i-1} \rho_i + \varepsilon_i \rho_{i-1}} \quad (22)$$

The first matrix in the right hand side of Eq. 21, called M , can be decomposed to two separate matrices called discontinuity matrix, $D_{i,i-1}$ and propagator matrix, T_{i-1} such that $M = D \times T$ where:

$$D_{i,i-1} = \begin{pmatrix} 1 & -\Delta_{i,i-1} \\ -\Delta_{i,i-1} & 1 \end{pmatrix} \quad (23)$$

and

$$T_{i-1} = \begin{pmatrix} 1 & 0 \\ 0 & e^{-2\rho_i d_{i-1}} \end{pmatrix} \quad (24)$$

Now, we can generalize this relation to any number of layers. We start at the leftmost layer L , and ending at the rightmost layer R with N layers in between and write[19]:

$$M = D_{R,N-1} \times T_{N-1} \times D_{N-1,N-2} \times T_{N-2} \times D_{N-2,N-3} \times T_{N-3} \times \cdots \times T_1 \times D_{1,L} \quad (25)$$

If in a periodic structure, $a_R^T = (A_R, B_R)$, $a_L^T = (A_L, B_L)$, and $a_R^T = M a_L^T$, then

$$A_R = m_{11}A_L + m_{12}B_L \quad (26)$$

$$B_R = m_{21}A_L + m_{22}B_L \quad (27)$$

But for incoming wave $B_L = 0$ and for outgoing wave $A_R = 0$ (see Eq.10). Therefore, $m_{11}A_L = 0$ and $B_R = m_{21}A_L$. Since, $A_L \neq 0$ then $m_{11} = 0$. The only excitations of the fields that satisfy the boundary conditions are those obtained from solving the secular equation $m_{11} = 0$ [19]. Also, in Lifshitz theory the fluctuation free energy is directly related to the m_{11} and is written as[19]

$$F(N, a, b) = k_B T \sum_q \sum_{n=0}^{\infty, \prime} \ln(m_{11}^{TE}) + k_B T \sum_q \sum_{n=0}^{\infty, \prime} \ln(m_{11}^{TM}) \quad (28)$$

where, k_B is Boltzmann constant and the primed sum signifies that the $n = 0$ term is taken with the weight

$1/2$ [19]. Sarlah et al., have shown that in a nonisotropic homogenous uniaxial slab composed of periodic layers, $F(N, a, b)$ can be written approximately as[29]:

$$F(N, a, b) = \frac{k_B T}{2\pi} \sum_{n=0}^{\infty, \prime} \int_0^\infty q dq \log(1 + \Delta_{RA} \Delta_{AL} e^{-2\rho_A(a+N(a+b))}) \quad (29)$$

where,

$$\Delta_{RA} = \frac{(\rho_A \varepsilon_A - \rho_A \varepsilon_\perp)}{(\rho_A \varepsilon_A + \rho_A \varepsilon_\perp)} = -\Delta_{AL} \quad (30)$$

and

$$\rho_A^2 = \frac{\varepsilon_\perp}{\varepsilon_\parallel} \left(q^2 - \frac{\varepsilon_\parallel \omega^2}{c^2} \right) \quad (31)$$

$$\varepsilon_\perp = \frac{1}{a+b} (a\varepsilon_A + b\varepsilon_B) \quad (32)$$

$$\varepsilon_\parallel = \frac{1}{a+b} (a/\varepsilon_A + b/\varepsilon_B) \quad (33)$$

We will use the Eq.29 for doing the numerical calculations. Finally, the dependency of interaction energy to the number of (AB) layers, (N) , is given by Hamaker coefficient $H(N, a, b)$ as[19]

$$H(N, a, b) = 12\pi(a+b)^2 F(N, a, b)/N^2 \quad (34)$$

D. Three-body photon heat amplification

Fig.2 shows a three-body configuration including silicon as leftmost and rightmost regions and a monolayer of MoS_2 as intermediate layer. It has been shown that, the evanescent part P_{ev} of the heat flow between two bodies is equal to[17, 18]:

$$P_{ev} = \frac{\hbar}{\pi^2 d^2} \int_0^\infty \omega d\omega (n_B(E, T_1) - n_B(E, T_2)) \times \int_0^\infty \gamma d\gamma \frac{Im(\varepsilon_1)Im(\varepsilon_2)}{(|(\varepsilon_1 + 1)(\varepsilon_2 + 1) - (\varepsilon_1 - 1)(\varepsilon_2 - 1)e^{-\gamma}|)^2} e^{-\gamma} \quad (35)$$

where, d is vacuum distance between two bodies, $\gamma = -2p\omega d/c$, ε_1 and ε_2 are dielectric constant, c is veloc-

ity of light, and $n_B(E, T_i) = [e^{\hbar\omega} - 1]^{-1}$. The relation of $p = |\hat{p}|$ is given in our previous work[18]. If the MoS_2 layer is absent, then[18]:

$$X_1 \equiv \int_0^\infty \gamma d\gamma \frac{Im(\varepsilon_1)Im(\varepsilon_2)}{(|(\varepsilon_1 + 1)(\varepsilon_2 + 1) - (\varepsilon_1 - 1)(\varepsilon_2 - 1)e^{-\gamma}|)^2} e^{-\gamma} = \int_0^\infty \gamma d\gamma \frac{Im(\varepsilon_1)Im(\varepsilon_2)}{(|(\varepsilon_{Si} + 1)^2 - (\varepsilon_{Si} - 1)^2 e^{-\gamma}|)^2} e^{-\gamma} \quad (36)$$

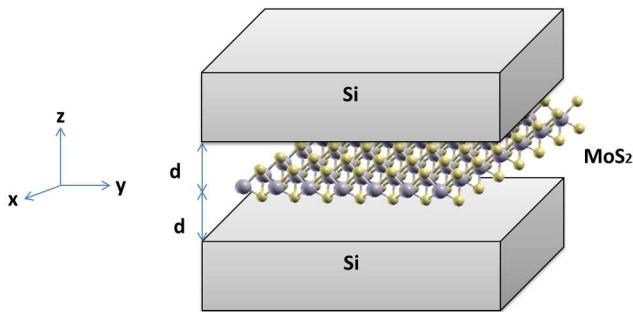


FIG. 2: (Color online) Three-body configuration including silicon as leftmost and rightmost regions and a monolayer of MoS_2 as intermediate layer.

where, $X = (n_B(E, T_1) - n_B(E, T_2)) \times X_1$ is radiative heat flux in the near-field and after normalization is shown by X^* [17, 18]. After adding the intermediate MoS_2 layer, its temperature is chosen such that the total heat flux on this layer is zero[18]. We will use the Eqs.35 and 36 for calculating the heat transfer in three-body configuration, shown in Fig.2.

III. RESULT AND DISCUSSION

A. Without gate voltage

Let us to start with dielectric constant of MoS_2 . Fig.3(a) shows the dielectric constant, ϵ , of monolayer MoS_2 via wavelength. Four peaks at $\lambda = 293, 451, 619,$ and $666nm$ are seen which is in good agreement with published data[27]. Now, we consider a multilayer structure of graphene and MoS_2 and study the photon tunneling across the structure in absence of gate voltage. First, we assume that, the layer A and layer B of Fig.1 are made by graphene (MoS_2), and MoS_2 (graphene), respectively. Fig.4(a) shows the interaction free energy across the structure via the number of layers, N .

As it is expected the free energy decreases by increasing the number of layers. It is well known that, the $TE(TM)$ mode of oscillations decays with factor $e^{-\gamma}$ from the surface of body[17, 18] and therefore, by increasing the distance between leftmost side and rightmost side, the free energy decrease. Also, the exponential term of Eq.29 depends on thickness of A-layer as $(N + 1)a$ and thickness of B-layer as Nb . The thickness of graphene and MoS_2 is $1 (A^0)$ and $3.1 (A^0)$, respectively[28, 30]. Therefore, when the first layer of stratified structure is MoS_2 the power of exponential term of Eq.29 is bigger than that of graphene. Then as Fig.4(a) shows, the free energy of $G/MoS_2/G$ is higher than $MoS_2/G/MoS_2$. Therefore, there is a general rule. The thinner layer should be the nearest neighborhood of leftmost and rightmost sides of stratified media for getting the highest interaction energy. Fig.4(b) shows the Hamaker coefficient via N . As it shows, the transition to the continuum approx-

imation begins from $N = 10$ for $G/MoS_2/G$ structure while it begins from $N = 5$ for $MoS_2/G/MoS_2$ structure. Therefore, from this point of view, the $MoS_2/G/MoS_2$ structure is better than $G/MoS_2/G$ structure.

B. With gate voltage

It has been shown that, the Fermi energy changes under applying the gate voltage (V_g), and in consequence, the absorption spectrum changes too[31, 32]. It means that, $\epsilon(\lambda)$, changes if an external gate voltage is applied. Fig. 3(b) shows, how $\epsilon(\lambda)$ changes via V_g . As it shows, the height of first peak decreases but the other peaks disappear when V_g is applied. Since, the heat photon tunneling between two bodies depends on the dielectric constant of bodies[17, 18] this property of monolayer MoS_2 can be used for tuning the tunneling phenomena. We study the effect of gate voltage on interaction free energy and Hamaker coefficient when $N = 1$. Fig.5(a) and (b) show the variation of interaction free energy and Hamaker coefficient via V_g for $T = 300$ Kelvin (K), respectively. As Eq.3 shows, for $V_g = 0 \rightarrow E_F = 0$, but the term $k_B T$ is not equal to zero in Eqs.4 and 5 and therefore, the value of free energy differs from the related value shown in Fig.4(a) when $V_g = 0$. This is the weakness point of the model. But as Fig.5(a) and (b) show, the both interaction free energy and Hamaker coefficient decrease by applying $V_g < -50$ eV due to the decreasing the dielectric constant of MoS_2 layer. Therefore, one is able to tune the interaction free energy by applying an external voltage.

C. Three-body configuration

In this section, we consider a three-body configuration, shown in Fig.2, and study the evanescent photon tunneling between two silicon layers in presence and absence of intermediate MoS_2 layer. We set the temperature of left side silicon at $T_1 = 1000K$ and right side silicon at $T_3 = 300K$. Then, we choose the temperature of intermediate MoS_2 layer at T_2 such that the heat flux is amplified between left and right silicon layers. Therefore, for doing that, we use the three-body amplification model[17, 18] instead of the above stratified media model. We use the data of Ref.33 for dielectric constant of silicon[33] (see Fig.6). Fig.7(a) shows the heat flux (in log-scale) between two silicon layers via distance between them (d) and wavelength (λ) when the temperature difference between layers is equal to $\Delta T = 700K$. As it shows, only for very small distance the heat flux has meaningful value. By adding the MoS_2 layer, coupling between modes is happened and heat is amplified between silicon layers[17, 18]. As Fig.7(b) shows, for some specific values of d and λ , the heat is amplified significantly. Now let us to apply the gate voltage and see what is happened. Fig.8 shows the heat flux via wave-

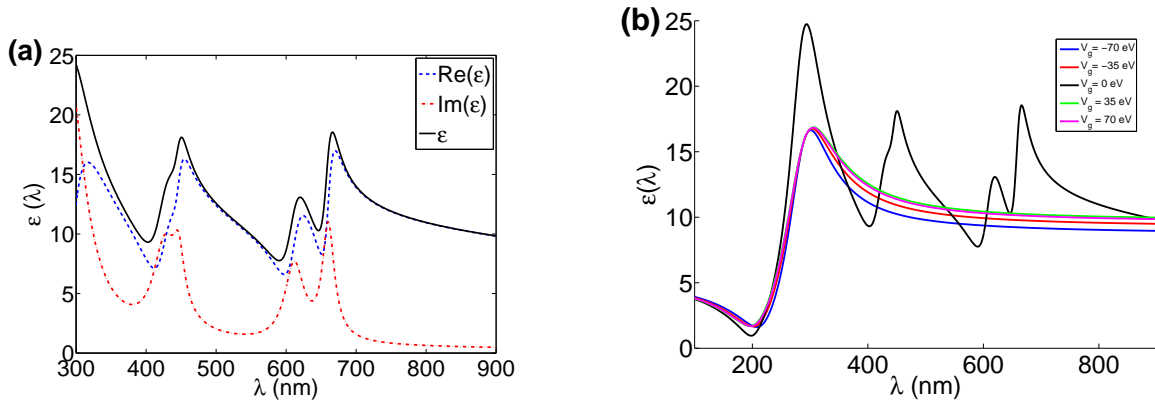


FIG. 3: (Color online) (a) The dielectric constant of (MoS_2) when $V_g = 0$ (eV) and (b) $V_g \neq 0$.

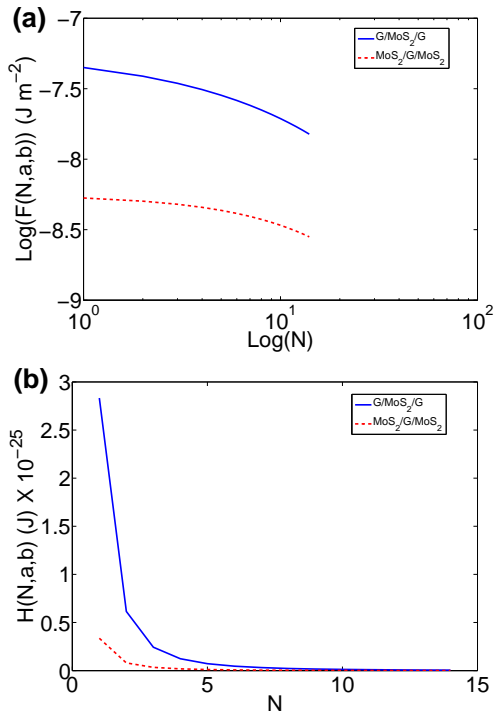


FIG. 4: (Color online) (a) The interaction free energy across N layers of MoS_2 (graphene) and $N + 1$ layers of graphene(MoS_2). The thickness of graphene and MoS_2 is equal to 1 and 3.1 Angstrom (A^0). (b) Hamaker coefficient via number of layers.

length when $d = 10nm$. As Fig.3(a) shows, three important peaks of dielectric constant of MoS_2 are placed at 451, 619, and 666 nm. As Fig.8(a) shows, For $V_g = 0$, two peaks of heat flux are placed at 602 and 654 nm and there is a valley at 425 nm, too. Therefore, it can be concluded that, the coupling between modes is happened at peaks, while, the destructive coupling causes the reduction of heat flux at valley. By applying the gate voltage, the destructive coupling is amplified and the peaks of heat

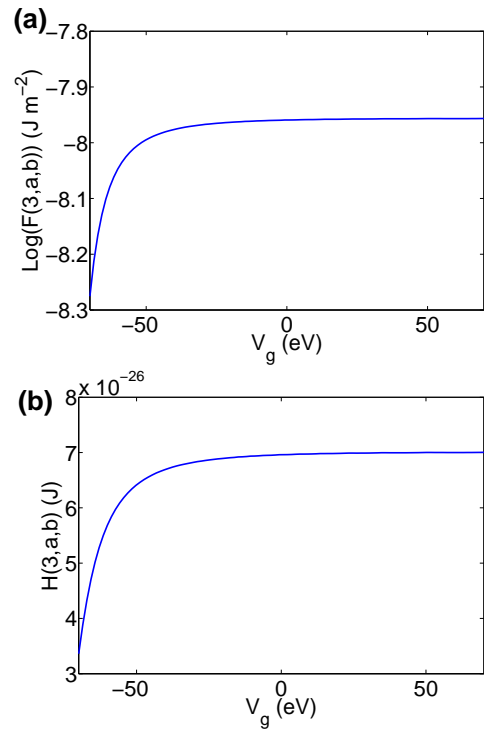


FIG. 5: (Color online) (a) The interaction free energy across one layer of MoS_2 and two layers of graphene and (b) Hamaker coefficient via gate voltage.

flux are disappeared (Fig.8(a)). As Fig.3(b) shows, the peaks of ϵ of MoS_2 are disappeared by applying the gate voltage. In consequence, as Fig.8(a) shows, by changing V_g , the heat flux changes and its peaks disappear. But as Fig.8(b) shows, there are differences between heat fluxes for different values of V_g . Therefore, we can tune the heat flux by applying the gate voltage. Since, the silicon is used for manufacturing near infrared detectors; the technique can be used for increasing the sensibility of this kind of detectors similar to the medium wavelength infrared detectors[34].

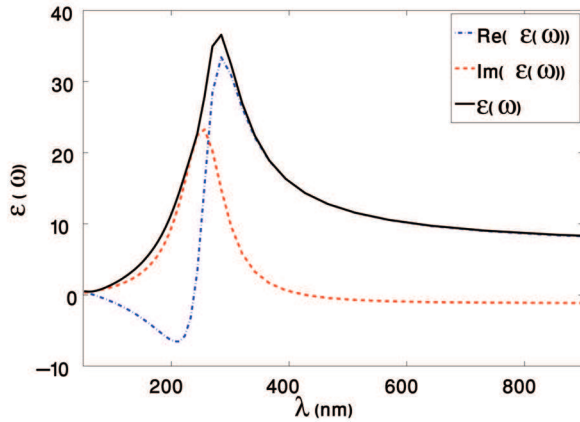


FIG. 6: (Color online) The dielectric constant of silicon.

IV. SUMMARY

We have considered a stratified media composed by graphene and MoS_2 layers and studied the interaction free energy in the media. We have shown that, when graphene is the nearest neighborhood of leftmost and rightmost side of the media, the interaction free energy is higher than that of MoS_2 due to the lower thickness of graphene. Therefore, it could be considered as a rule. It has been shown that, the evanescent heat flux between two silicon layers is amplified if an monolayer of MoS_2 is placed between them. By applying a gate voltage to the intermediate MoS_2 layer, we have shown that, the heat flux between silicon layers could be tuned, and in consequence, the technique can be used for increasing the sensibility of near infrared detectors.

-
- [1] J. E. Sipe, J. Opt. Soc. Am. B **4**, 4 (1987).
 [2] J. J. Loomis and H. J. Maris, Phys. Rev. B **50**, 24 (1994).
 [3] A. Narayanaswamy and G. Chen, J. Quant. Spect. Radiat. Trans. **111**, 1877 (2010).
 [4] A. Narayanaswamy and G. Chen, J. Quant. Spect. Radiat. Trans. **132**, 12 (2014).
 [5] K. Joulain, J. P. Mulet, F. Marquier, R. Carminati, and J. J. Greffet, Surf. Sci. Rep. **57**, 59 (2005).
 [6] A. I. Volokitin and B. N. J. Persson, Rev. Mod. Phys. **79**, 1291 (2007).
 [7] M. D. Whale, *A Fluctuational Electrodynamics Analysis of Microscale Radiation Transfer and the Design of Microscale Thermophotovoltaic Devices* (Pergamon, New York, 1997).
 [8] D. Polder and M. Vanhove, Phys. Rev. B **4**, 3303 (1971).
 [9] J. P. Mulet, K. Joulain, R. Carminati, and J. J. Greffet, Microscale Thermophys. Eng. **6**, 209 (2002).
 [10] C. J. Fu and Z. M. Zhang, Int. J. Heat Transfer **49**, 1703 (2006).
 [11] J. P. Mulet, K. Joulain, R. Carminati, and J. J. Greffet, Opt. Lett. **26**, 280 (2001).
 [12] J. L. Pan, Opt. Lett. **26**, 482 (2001).
 [13] S. Basu, B. J. Lee, and Z. M. Zhang, ASME Trans. J. Heat Transfer (unpublished).
 [14] A. I. Volokitin and B. N. J. Persson, Phys. Rev. B **63**, 205404 (2002).
 [15] P. O. Chapuis, S. Volz, C. Henkel, K. Joulain, and J. J. Greffet, Phys. Rev. B **77**, 035431 (2008).
 [16] S. Basu and Z. M. Zhang, J. Appl. Phys. **105**, 093535 (2009).
 [17] R. Messina, M. Antezza, and P. Ben-Abdallah, Phys Rev Lett. **109**, 224302 (2012).
 [18] H. Simchi, (2016), cond-mat.mes-hall/1611.03801v1.
 [19] R. Podgornik, P. L. Hansen, and V. A. Parsegian, J. Chem. Phys. **119**, 2 (2003).
 [20] R. Podgornik and V. A. Parsegian, J. Chem. Phys. **120**, 7 (2004).
 [21] X. Zhang, D. O. Hayward, and D. M. P. Mingos, Catal. Lett. **84**, 225 (2002).
 [22] S. Kim, A. Konar, W. S. Hwang, J. H. Lee, J. Lee, J. Yang, C. Jung, H. Kim, J. B. Yoo, and Y. J. Choi, Nat Commun. **3**, 1011 (2012).
 [23] M. G. Bell and Y. W. Liang, Adv. Phys. **1976**, 53 (1976).
 [24] R. F. Frindt and A. D. Yoffe, Proc. R. Soc. London, Ser. A **273**, 69 (1963).
 [25] A. R. Beal and H. P. Hughes, J. Phys. C: Solid State Phys. **12**, 881 (1979).
 [26] E. J. G. Santos and E. Kaxiras, ACS Nano **7**, 12 (2013).
 [27] B. Mukherjee, F. Tseng, D. Gunlycke, K. K. Amara, G. Eda, and E. Simsek, Opt. Matt. Expr. **5**, 2 (2015).
 [28] J. Sarabadani, A. Naji, R. Asgari, and R. Podgornik, (2011), cond-mat.mes-hall/1105.4241v1.
 [29] A. Sarlah and S. Zumer, Phys. Rev. E **64**, 051606 (2001).
 [30] Z. M. Wang, *MoS2: Materials, Physics, and Devices* (Springer, 2014).
 [31] A. K. M. Newaz, D. Prasai, G. I. Ziegler, D. Caudel, S. Robinson, R. F. Haglund, and K. L. Bolotin, Solid State Commun. **155**, 49 (2013).
 [32] Z. Li, S. W. Chang, C. C. Chen, and S. B. Cronin, Nano research **7**, 973 (2014).
 [33] J. P. Walter and M. L. Cohen, Phys. Rev. B **5**, 8 (1972).
 [34] R. Messina and P. Ben-Abdallah, Sci. Rep. **3**, 1383 (2013).

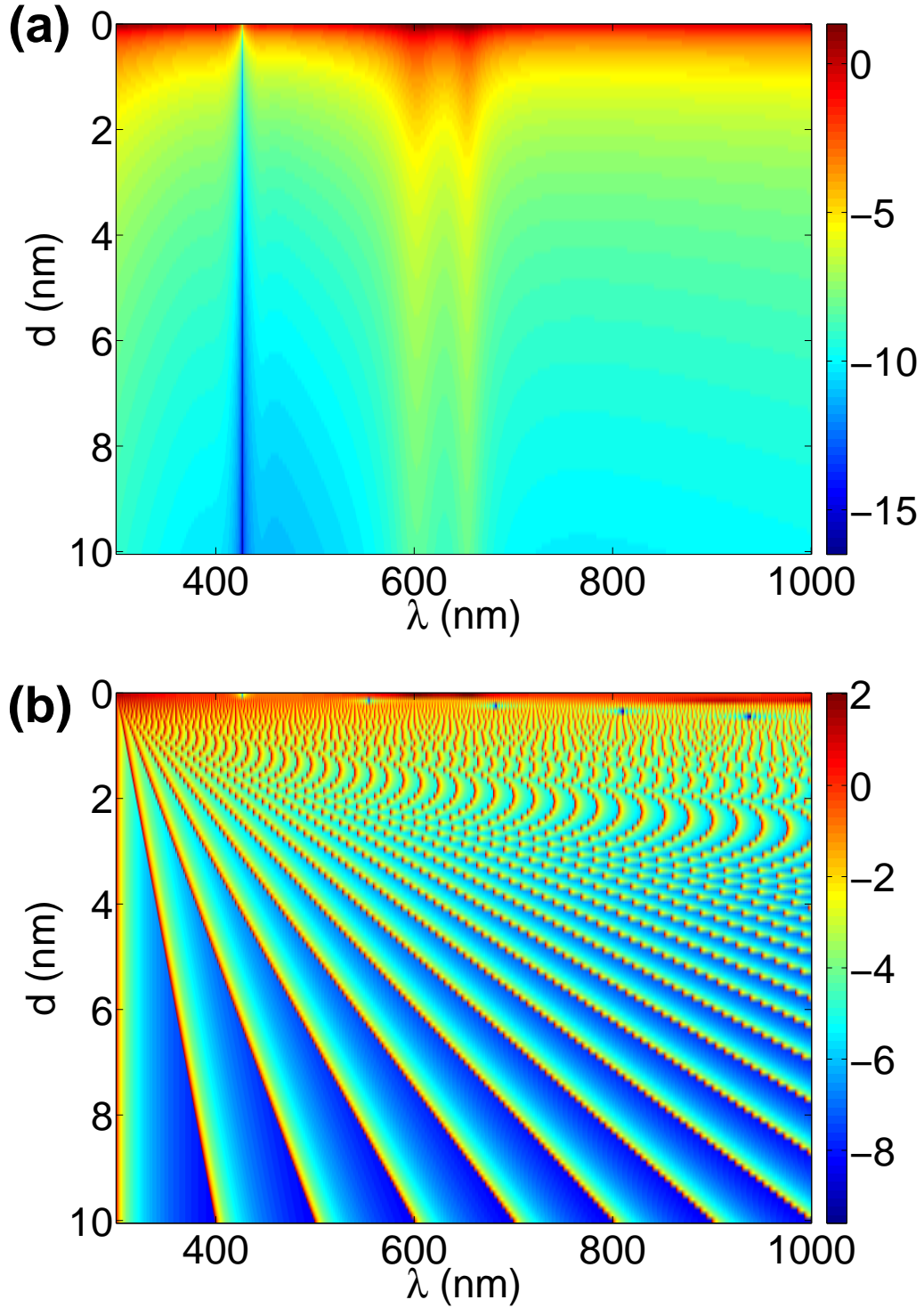


FIG. 7: (Color online) (a) $\text{Log}(X^*)$ via distance between two silicon layers, d , and wavelength λ , when $T_1 = 1000K$ and $T_2 = 300K$. (b) $\text{Log}(X^*)$ via distance between each layer and intermediate MoS_2 layer, d , and wavelength λ , when $T_1 = 1000K$ and $T_3 = 300K$. The temperature of MoS_2 layer (T_2) should be tuned (see text).

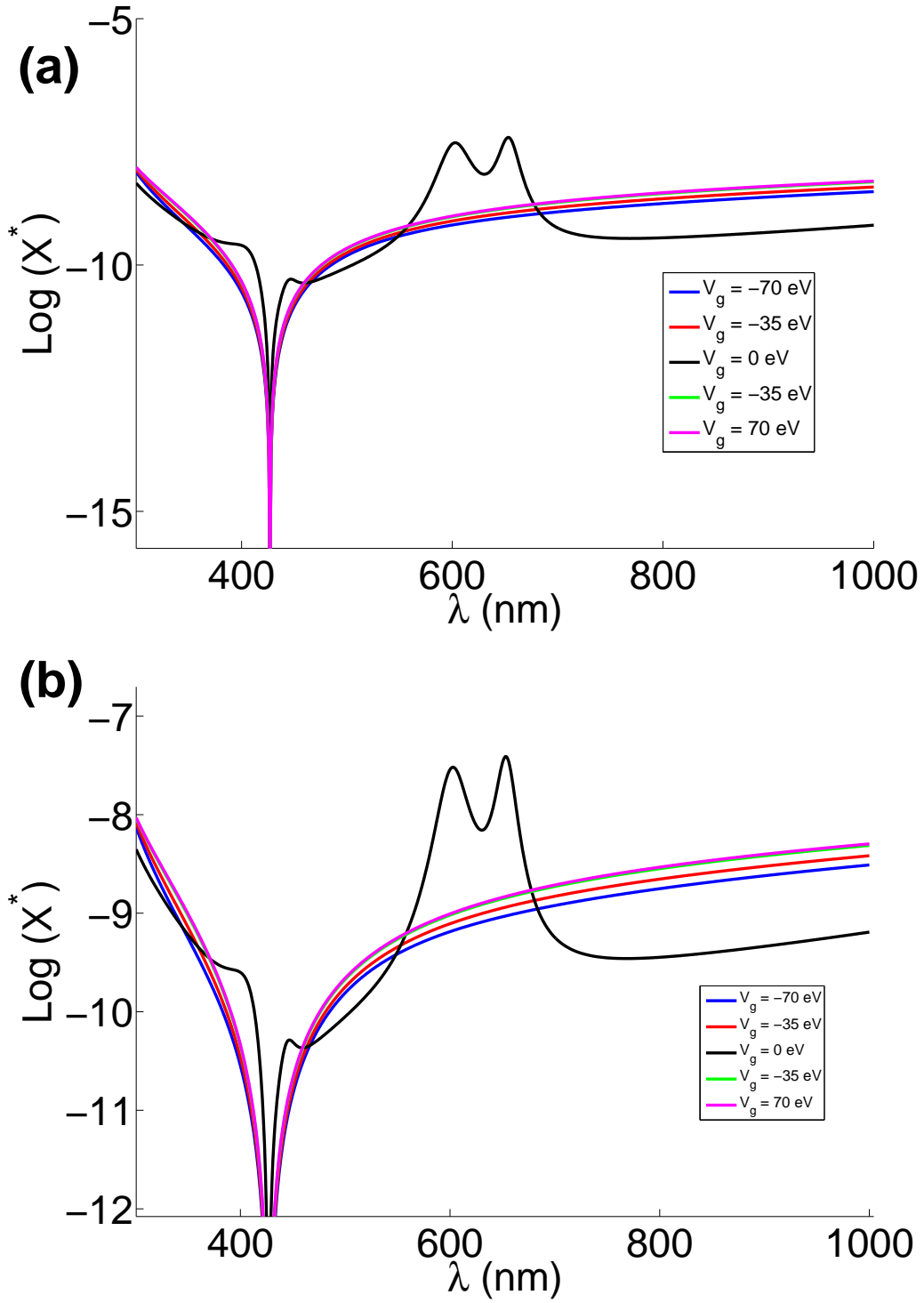


FIG. 8: (Color online) (a) $\text{Log}(X^*)$ via wavelength λ , when the distance between silicon layer and MoS_2 layer, $d = 10\text{nm}$, and $T_1 = 1000\text{K}$, $T_3 = 300\text{K}$ and The temperature of MoS_2 layer (T_2) is tuned (see text). (b) inset of Fig.8(a).